

**Thermal annealing of C ion irradiation defects in nuclear graphite studied by positron annihilation**

Shi, C. Q.; Schut, H.; Li, Z. C.

**DOI**

[10.1088/1742-6596/674/1/012019](https://doi.org/10.1088/1742-6596/674/1/012019)

**Publication date**

2016

**Document Version**

Final published version

**Published in**

Journal of Physics: Conference Series

**Citation (APA)**

Shi, C. Q., Schut, H., & Li, Z. C. (2016). Thermal annealing of C ion irradiation defects in nuclear graphite studied by positron annihilation. *Journal of Physics: Conference Series*, 674(1), Article 012019. <https://doi.org/10.1088/1742-6596/674/1/012019>

**Important note**

To cite this publication, please use the final published version (if applicable). Please check the document version above.

**Copyright**

Other than for strictly personal use, it is not permitted to download, forward or distribute the text or part of it, without the consent of the author(s) and/or copyright holder(s), unless the work is under an open content license such as Creative Commons.

**Takedown policy**

Please contact us and provide details if you believe this document breaches copyrights. We will remove access to the work immediately and investigate your claim.

PAPER • OPEN ACCESS

## Thermal annealing of C ion irradiation defects in nuclear graphite studied by positron annihilation

To cite this article: C Q Shi *et al* 2016 *J. Phys.: Conf. Ser.* **674** 012019

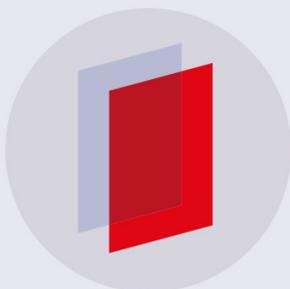
View the [article online](#) for updates and enhancements.

### Related content

- [Nanostructures of carbon in nuclear graphite](#)  
K Y Wen, J Marrow and B J Marsden
- [Thermal annealing induced modification of structural and soft magnetic properties of Fe<sub>33.8</sub>Co<sub>50.7</sub>Nb<sub>5</sub>B<sub>8.5</sub>P<sub>2</sub> alloy](#)  
M Shah, S S Modak, N Ghodke *et al.*
- [Effects of post-growth thermal annealing on room temperature pulsed laser deposited ZnO thin films](#)  
D Padilla Rueda, J M Vadillo and J J Laserna

### Recent citations

- [Interlayer vacancy defects in AA-stacked bilayer graphene: density functional theory predictions](#)  
A Vuong *et al*



**IOP | ebooks™**

Bringing you innovative digital publishing with leading voices to create your essential collection of books in STEM research.

Start exploring the collection - download the first chapter of every title for free.

# Thermal annealing of C ion irradiation defects in nuclear graphite studied by positron annihilation

C Q Shi<sup>1</sup>, H Schut<sup>2</sup> and Z C Li<sup>1,3,4</sup>

<sup>1</sup> State Key Lab of New Ceramic and Fine Processing, School of Materials Science & Engineering, Tsinghua University, Beijing, China

<sup>2</sup> Department of Radiation Science and Technology, Delft University of Technology, Mekelweg 15, 2629 JB Delft, the Netherlands

<sup>3</sup> Key Laboratory of Advanced Materials (MOE), School of Materials Science & Engineering, Tsinghua University, Beijing, China

Email: zcli@tsinghua.edu.cn

**Abstract.** In order to investigate the thermal behaviour of radiation induced point defects in nuclear graphite, ETU10 graphite was implanted with 350 keV C<sup>+</sup> ion to doses of 10<sup>15</sup> and 10<sup>16</sup> cm<sup>-2</sup>. The point defects introduced by the implantation were characterized by Positron Annihilation Doppler Broadening (PADB) and their thermal behaviour was studied during “in situ” annealing at Delft Variable Energy Positron beam (VEP). The annealing was performed for 5 minutes at temperatures ranging from 300 K (as implanted) to 1500 K in steps of 100 K. For both doses, an annealing stage at around 450 K is observed followed by a second stage around 700 K. For the high dose implantation vacancy complexes are found which are stable up to a temperature around 1400K.

## 1. Introduction

Since the building of the first gas-cooled nuclear reactors, graphite has been classified as one of the most promising moderator candidates because of its low atomic number, high thermal conductivity and good mechanical properties[1]. Apart from the moderator function, this material could also be used as reflector and structural materials in the reactor core, which makes nuclear graphite one of the key nuclear materials in the nuclear industry[2]. As a complex polygranular system, nuclear graphite consists two phases: a filler material and a binder phase. The most common filler material is petroleum coke made by delayed coking process[3]. The typically used binder phase in the manufactory is coal tar pitch. After a final stage of graphitization, a very high chemical purity is reached[4]. However, the service performance of nuclear graphite would be greatly impaired as a result of the collision events with fast neutrons, which will lead to the formation of structural defects such as displaced atoms, vacancies and interstitial loops or vacancy aggregations. In addition, Ewel et al also suggested the formation of metastable interstitial-vacancy pair structure in the irradiated nuclear graphite[5]. The subsequent evolution of these defects will lead to dimensional and physical properties changes and the release of the Wigner energy, which is detrimental to the safety of the reactor[6]. Over the past decades, understanding of these defects and their behaviour have always been a front area of the graphite research field[7]. In particular, the behaviour of radiation induced point defects is of technical and scientific interest. Characterization techniques such as transmission electron microscopy (TEM),

<sup>4</sup> To whom any correspondence should be addressed.



scanning tunnelling microscopy (STM) supported by computer simulations[8-10] have greatly enhanced the knowledge about irradiation induced damage of graphite. However, it is still not quite clear what mechanisms play a role in the defect behaviour at atomic level. In this work the nuclear graphite ETU10 was implanted with 350 keV C<sup>+</sup> ions to simulate the collision events with neutrons.

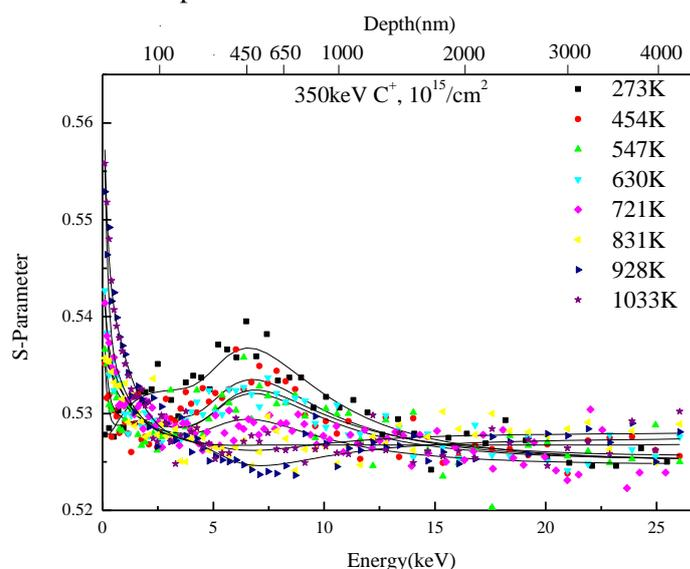
## 2. Experimental

The samples were manufactured by IBIDEN. It has an apparent density of 1.75 g/cm<sup>3</sup> with low porosity of 15%, and it has a very low ash content of less than 5 ppm. The thermal conductivity is 104.4 W/mK, and the thermal expansion is  $3.8 \times 10^{-6} \text{ K}^{-1}$ . Two pieces of nuclear graphite ETU10 (20x20x2mm<sup>3</sup>), were implanted with 350 keV C<sup>+</sup> ions to doses of 10<sup>15</sup> and 10<sup>16</sup> /cm<sup>2</sup>, respectively. During the implantations carried out at the Institute of Semiconductors, Chinese Academy of Science, Beijing, the temperature of the samples was kept below 373K.

The point defects introduced by the implantation and their thermal behavior were characterized by the Positron Annihilation Doppler Broadening (PADB) technique at Delft Variable Energy Positron beam (VEP). By selecting positron implantation energies between 0.1 and 25 keV, the maximum obtained positron mean implantation depth is 4 μm. This is well beyond the 1 μm range of the displacement damage distribution (with a 200 nm wide maximum at about 700 nm depth) predicted by SRIM [11]. The “in situ” annealing was performed for 5 minutes at temperatures ranging from 273 K (as implanted) to 1500 K in steps of 100 K. The PADB experiments were started after the samples had cooled down to RT. The measured Doppler broadening S-parameters are calculated as the ratio of the counts registered in a fixed momentum window, with  $|p_{\parallel}| < 3.5 \times 10^{-3} m_0c$ , to the total number of counts in the 511 keV photon peak. Here  $p_{\parallel}$  is the momentum of the electrons in the direction of gamma emission,  $m_0$  is the electron rest mass and  $c$  is the speed of light.

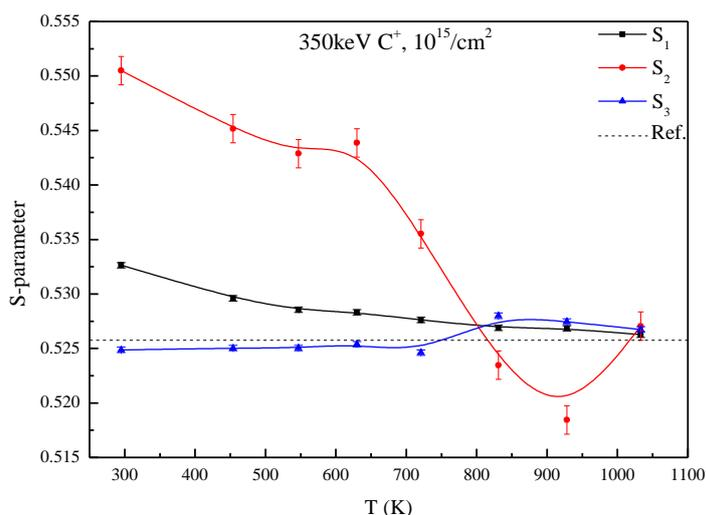
## 3. Results and Discussion

Figure 1 shows the results of the PADB experiments after stepwise annealing of ETU10 irradiated with 10<sup>15</sup> C<sup>+</sup>/cm<sup>2</sup>. For clarity reasons the S value of the as-received ETU10 as reference is shown in Figure 3. It has to be clarified that in the interest of a concise plot, the error bars are only shown in Figure 3 for the reference and the first PADB measurement. Based on the same measurement principle, the lengths of the error bars are expected to be at the similar scale for the rest data in Figures 1 and 3.



**Figure.1** S-Parameter versus positron energy for ETU10 implanted with 10<sup>15</sup> C<sup>+</sup>/cm<sup>2</sup>

For the as-received ETU10 specimen, it can be seen that the  $S$  values distribute randomly between 0.520 and 0.530, which indicates that positrons show no significant depth preference when annihilate within the penetration range. Therefore, we could take this as the reference when compared with the as-irradiated data. In Figures 1 and 3 the latter is displayed by the scatter symbols, while the full lines through the symbols are the results of VEPFIT[12] calculations using a three-layer-model. The width of the first two layers is derived from the SRIM calculations. The mean implantation depth scale of positron is shown on the top of the chart. The expression of the calculation is described elsewhere[13]. The first layer extends up to 450 nm beneath the implantation surface followed by the second layer with a width of 200 nm. The third and last layer covers the range up to the maximum positron implantation depth and represents the undamaged region. Thus,  $S_1$ ,  $S_2$ ,  $S_3$  are the fitted Doppler broadening parameters of the first, second layer and the bulk, respectively. As can be seen, the data of the “as-implanted” sample (273 K) shows a maximum of about 0.54 at the positron implantation energy of about 7 keV. This energy corresponds to a mean positron implantation depth of about 500 nm. This maximum is well above the average value of 0.525 found for the non-implanted region, and therefore is representative for defects introduced by the carbon ion irradiation. With increasing annealing temperature the maximum in the  $S$  curve decreases to the level obtained for the reference sample. Figure 2 shows the values of the fitted Doppler parameters ( $S_1$ ,  $S_2$  and  $S_3$ ) as a function of annealing temperature.



**Figure 2.** Fitted  $S$  values as a function of the annealing temperature. The uncertainties in the fitted parameters are obtained by VEPFIT.

The clear drop of the  $S_2$  value after annealing at 450 K is consistent with the well accepted Wigner energy release at about 473 K[14]. This could be interpreted as the annihilation of the Frenkel pair defects, that is, the vacancies are mobile at 473 K to annihilate adjacent interstitial[15]. At annealing temperatures between 450 K and 600K, the  $S$ -parameter decreases slowly while a next sharp decrease is observed at 700 K. As Wigner energy may release at different stages, the significant reduction may result from more released Wigner energy. Accompanied by the energy release, the most possible internal process is the monovacancy migration and in case of high vacancy density aggregation into multi-vacancy complexes, which could only be removed by elevated annealing temperature[15]. A next sharp decrease is observed at annealing temperature higher than 700K where after  $S_2$  decreases quickly to the bulk  $S$  value. For the moment (based on the Doppler broadening data only) it is difficult to explain the low  $S_2$  value at the temperature around 900 K. Usually, a low  $S$  parameter is associated with small open-volumes, and an  $S$  parameter lower than that of the reference would hint at volumes

smaller than that associated with interstitial dimensions. Possibly, this could be verified by future positron annihilation lifetime experiments. The Doppler parameter  $S_1$  representing the near surface defects, is less influenced by the implantation and the effect of annealing is observed as a gradual decrease without evidence of annealing stages. Apparently, almost all the defects (monovacancies) have been removed, which shows that defects induced by low dose ion irradiation can be easily removed at lower annealing temperature. Figure 3 presents the PADB measurements of ETU10 irradiated at a ten times higher C ion dose of  $10^{16}/\text{cm}^2$ . The observed higher maximum of the S-parameter indicates that more defects (or larger open volume defects) are introduced. In addition, an increase of S in the first near surface layer is clearly present.

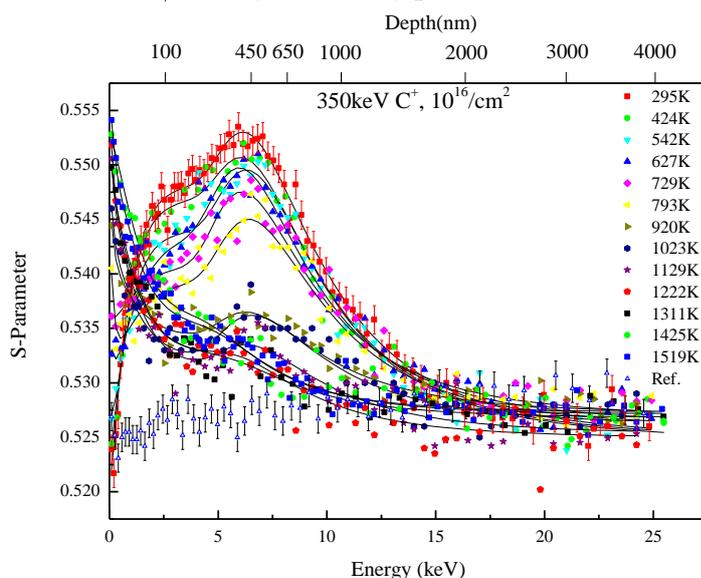


**Figure 3.** S-Parameter versus positron energy for ETU10 implanted with  $10^{16} \text{ C}^+/\text{cm}^2$ .

Figure 4 shows the values of the fitted Doppler parameters ( $S_1$ ,  $S_2$  and  $S_3$ ) as a function of annealing temperature. (Note the extended temperature scale in comparison to figure 2).

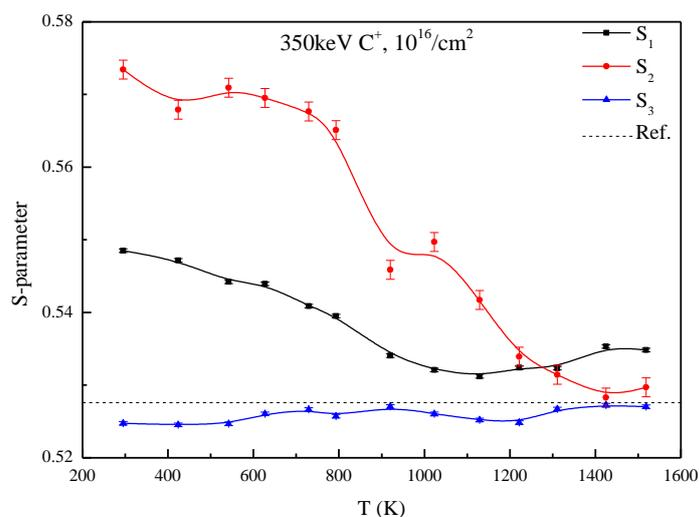


**Figure 4.** Fitted S values as a function of the annealing temperature.

As in the case of the dose of  $10^{15}/\text{cm}^2$ , the first annealing stage in  $S_2$  is seen at a temperature 400 K, which also derives from the characteristic Wigner energy release. With the annealing temperature increasing to 800 K, the  $S_2$  value descends gradually, followed by a sharp decrease between 800K and 920 K. In case of the low dose implantation at this temperature the majority of the small vacancy defects have been annealed out. For the high dose implantation this is clearly not the case and therefore the annealing was continued. At the next annealing temperature of about 1000K first an increase in  $S_2$  is observed. It is noteworthy that a similar increase is seen in the analyses of the low dose implanted sample. In this case the increase started from a lower level associated with the bulk. Further annealing results in a gradual decrease in  $S$  towards the bulk value. However, the maximum in the  $S$  curve is still higher than that of the reference data. Tang[16] suggests an aggregation structure formed by 6 vacancies as the possible stable cluster in heavily irradiated graphite. The planar  $V_6$  rings may survive even at temperature up to 1773 K as seen in this study.

The annealing behaviour of  $S_1$  for the high dose implantation shows a trend similar to that of  $S_2$  for the low dose in which the effect of vacancy clustering is less pronounced because of the lower initial vacancy concentration. The exception is that in the near surface region the bulk value is not fully reached. A similar effect is seen in our recent studies on 200 keV He irradiated nuclear graphite [17] and may be caused by surface erosion by ion impact.

#### 4. Conclusion

Defects in nuclear graphite ETU10 have been introduced by 350 keV C-ion implantation to doses of  $10^{15}$  and  $10^{16}$   $\text{C}^+/\text{cm}^2$ , respectively. The thermal evolution of the point defects has been studied by Positron Annihilation Doppler Broadening after “in situ” annealing up to 1500 K. For both doses an annealing stage at around 450 K is observed followed by a second stage around 700 K. For the high dose implantation vacancy complexes are found which are stable up to a temperature around 1400K.

#### Acknowledgments

The authors are grateful to the Koninklijke Nederlandse Akademie van Wetenschappen (KNAW, the Netherlands), the National Science and Technology Major Project (under Grant 2011ZX06901-017 and 2008ZX06901-001, China), and the National Natural Science Foundation of China (under Grant 61176003, China). We thank Professor Tadashi Maruyama of Tokyo Institute of Technology for providing graphite samples and the necessary information about the samples.

#### References

- [1] Marsden B J, Wickham A J 2006 *IAEA TECDOC-1521*
- [2] Chen D Y, Li Z C, Miao W, Zhang Z 2012 *Mater. Trans.* **53** 1159
- [3] Burchell T.D. 2012 *Material Properties/Oxide Fuels for Light Water Reactors and Fast Neutron Reactors* (Comprehensive Nuclear Materials vol.2, Amsterdam: Elsevier)
- [4] Zhou Z, Bouwman W G, Schut H, Pappas C 2014 *Carbon* **69** 17
- [5] Telling R H, Heggie M I 2007 *Philos. Mag.* **87** 4797
- [6] Ewels C P, Telling R H, El-Barbary A A, Heggie M I, Briddon P R 2003 *Phys. Rev. Lett.* **91** 025505
- [7] Banhart F 1999 *Rep. Prog. Phys.* **62** 1181
- [8] Bollmann W 1961 *J. Appl. Phys.* **32** 869
- [9] Liu J, Yao H J, Sun Y M, Duan J L, Hou M D, Mo D, Wang Z G, Jin Y F, Abe H, Li Z C, Sekimura N 2006 *Nucl. Instrum. Methods Phys. Res. B* **245** 126
- [10] Muto S, Horiuchi S, Tanabe T 1999 *J. Electron Microsc.* **48** 767
- [11] Ziegler J F, Biersack J P, Ziegler M D 2008 *SRIM - The Stopping and Range of Ions in Matter* (Chester, Maryland: SRIM Company)
- [12] Veen A van, Schut H, Clement M, Nijs J M M de, Kruseman A, Ijpma M R, 1995 *Appl. Surf. Sci.* **85** 216

- [13] Carvalho I, Schut H, Fedorov A, Luzginova N, Sietsma J 2013 *J. Nucl. Mater.* **442** S48
- [14] Mitchel E W J and Taylor M R 1965 *Nature* **208** 638
- [15] Latham C D, Heggie M I, Alatalo M, Öberg S, Briddon P R 2013 *J. Phys. Condens. Matter* **25** 135403
- [16] Tang Z, Hasegawa M, Shimamura T, Nagai Y, Chiba T, Kawazoe Y, Takenaka M, Kuramoto E, Iwata T 1999 *Phys. Rev. Lett.* **82** 2532
- [17] Hu Z, Li Z C, Zhou Z, Shi C Q, Schut H, Katia P 2014 *J. Phys.: Conf. Ser.* **505** 012014